
Neural encoding with visual attention

Meenakshi Khosla^{*}, Gia H. Ngo¹, Keith Jamison³, Amy Kuceyeski^{3,4} and Mert R. Sabuncu^{1,2,3}

¹ School of Electrical and Computer Engineering, Cornell University, Ithaca, NY 14853

² Nancy E. and Peter C. Meinig School of Biomedical Engineering, Cornell University, Ithaca, NY 14853

³ Radiology, Weill Cornell Medicine, New York, NY 10065

⁴ Brain and Mind Research Institute, Weill Cornell Medicine, New York, NY 10065

Abstract

Visual perception is critically influenced by the focus of attention. Due to limited resources, it is well known that neural representations are biased in favor of attended locations. Using concurrent eye-tracking and functional Magnetic Resonance Imaging (fMRI) recordings from a large cohort of human subjects watching movies, we first demonstrate that leveraging gaze information, in the form of attentional masking, can significantly improve brain response prediction accuracy in a neural encoding model. Next, we propose a novel approach to neural encoding by including a trainable soft-attention module. Using our new approach, we demonstrate that it is possible to learn visual attention policies by end-to-end learning merely on fMRI response data, and without relying on any eye-tracking. Interestingly, we find that attention locations estimated by the model on independent data agree well with the corresponding eye fixation patterns, despite no explicit supervision to do so. Together, these findings suggest that attention modules can be instrumental in neural encoding models of visual stimuli.

1 Introduction

Developing accurate population-wide neural encoding models that predict the evoked brain response directly from sensory stimuli has been an important goal in computational neuroscience. Modeling neural responses to naturalistic stimuli, in particular stimuli that reflect the complexity of real-world scenes (e.g., movies), offers significant promise to aid in understanding the human brain as it functions in everyday life [1]. Much of the recent success in predictive modeling of neural responses is driven by deep neural networks trained on tasks of behavioral relevance. For example, features extracted from deep neural networks trained on image or auditory recognition tasks are currently the best predictors of neural responses across visual and auditory brain regions, respectively [2, 3, 4]. While this success is promising, the unexplained variance is still large enough to prompt novel efforts in model development for this task. One aspect that is often overlooked in existing neural encoding models in vision is visual attention.

Natural scenes are highly complex and cluttered, typically containing a myriad of objects. What we perceive upon viewing complex, naturalistic stimuli depends significantly on where we direct our attention. It is well known that multiple objects in natural scenes compete for neural resources and attentional guidance helps to resolve the ensuing competition [5]. Due to the limited information processing capacity of the visual system, neural activity is biased in favor of the attended location [6, 7]. Hence, more salient objects tend to be more strongly and robustly represented in our brains. Further, several theories have postulated that higher regions of the visual stream encode increasingly shift- and scale-invariant representations of attended objects after filtering out interference from

*Correspondence: mk2299@cornell.edu

surrounding clutter [8, 9]. These studies suggest that deployment of attention results in an information bottleneck, permitting only the most salient objects to be represented in the inferotemporal (IT) cortex, particularly the ventral visual stream which encodes object identity. These findings together indicate that visual attention mechanisms can be crucial to model neural responses of the higher visual system.

Visual attention and eye movements are tightly interlinked. Where we direct our gaze often quite accurately signals the focus of our attention [10]. This form of attention, known as overt spatial attention, can be directly measured by eye-tracking. Recent work has shown that fMRI activity can be used to directly predict fixation maps or eye movement patterns under free-viewing of natural scenes, suggesting a strong link between neural representations and eye movements [11]. More recent large-scale efforts in such concurrent data collection, such as the Human Connectome Project (HCP) [12], that simultaneously record fMRI and eye-tracking measurements on a large population under free-viewing of movies, present a novel opportunity to probe the potential role of attention in neural encoding models of ecological stimuli.

Our contributions in this study are as follows:

- We demonstrate that leveraging information about attended locations in an input image can be helpful in predicting the evoked neural response. Particularly, we show that attentional masking of high-level stimulus representations based on human fixation maps can dramatically improve neural response prediction accuracy for naturalistic stimuli across large parts of the cortex.
- We show that it is possible to use supervision from neural response prediction solely to co-train a visual attention network. This training strategy thus encourages only those salient parts of the image to dominate the prediction of the neural response. We find that the neural encoding model with this trained attention module outperforms encoding models with no or fixed attention.
- Interestingly, we find that despite not being explicitly trained to predict fixations, the attention network within the neural encoding model compares favorably against saliency prediction models that aim to directly predict likely human fixation locations given an input image. This suggests that neural response prediction can be a powerful supervision signal for learning where humans attend in cluttered scenes with multiple objects. This signals a novel opportunity for utilizing functional brain recordings during free-viewing to understand visual attention.

2 Methods

Neural encoding models comprise two major components: a representation (feature extraction) module that extracts relevant representations from raw stimuli and a response model that predicts neural activation patterns from the feature space. We propose to integrate a trainable soft-attention module on top of the representation network to learn attention schemes that guide the prediction of whole-brain neural response. Our proposed methodology is illustrated in Figure 1.

Feature extraction network We employ the state-of-the-art ResNet-50 [13] architecture pre-trained for object recognition on ImageNet [14] as the representation network to extract semantically rich features from raw input images. In this study, we focus on improving neural response prediction in higher-order regions of the visual pathway where receptive fields are larger and not limited to a single hemi-field. Prior evidence suggests that these regions are likely best modelled by deeper layers of object recognition networks [3, 15]. Thus, we extract the output of the last "residual block", namely res5 (after addition) before the global pooling operation to encode all images into a 2048-channel high-level feature representation image (of size 23×32 , in our experiments), denoted as F_{rep} . All pre-trained weights are kept frozen during training of the neural encoding models.

Attention network The attention network operates on the 2048-channel feature representation image F_{rep} . For simplicity, we employed a single convolutional layer that constructs the saliency map with a trainable 5×5 filter $V_{att} \in \mathbb{R}^{5 \times 5 \times 2048 \times 1}$ as, $S = G_\sigma * [V_{att} * F_{rep}]_+$. Here, $|\cdot|_+$ denotes the ReLU operation and $G_\sigma *$ indicates blurring using a 5×5 gaussian kernel with $\sigma = 1$. The attention scores for each pixel are finally computed from saliency maps by normalizing with the

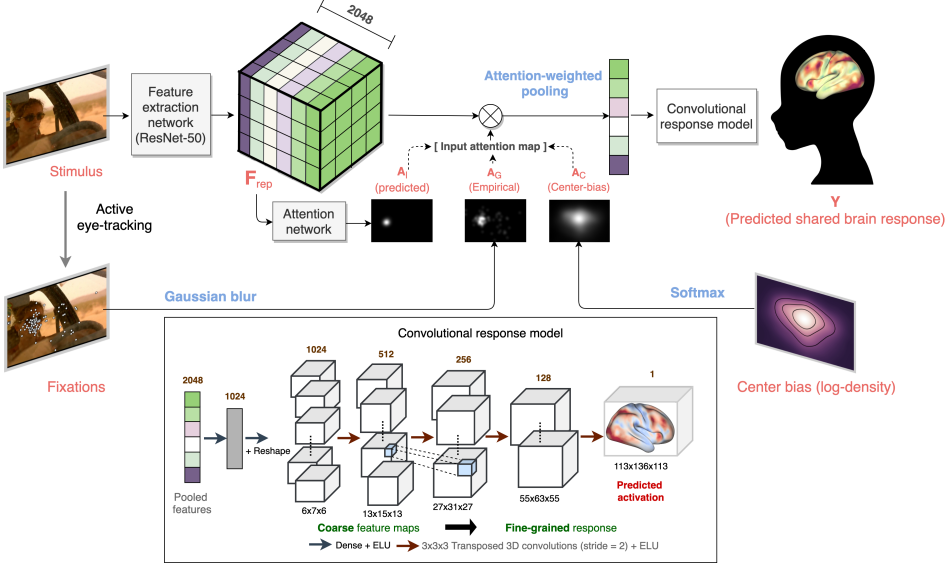


Figure 1: Proposed method. A trainable soft-attention module is implemented on top of a pre-trained representation network to rescale features based on their salience. The rescaled features are spatially pooled and fed into a convolutional response model to predict whole-brain neural response. We assess the value of the trained attention network by comparing it with neural encoding methods employing (i) stimulus-dependent attention maps derived from human fixations (A_G), (ii) stimulus-independent attention map derived from all fixations in the training set that reflects the center-weighted bias of our dataset (A_C) as well as a (iii) no attention model that spatially pools the features directly with no scaling.

spatial softmax operation,

$$A_l^{(i)} = \frac{\exp S^{(i)}}{\sum_{j=1}^n \exp S^{(j)}}, i \in \{1, \dots, n\}. \quad (1)$$

Here, superscript i is used to index the 23×32 spatial locations in the feature map F_{rep} . We note that existing literature on selective visual attention suggests a hierarchical winner-take-all mechanism for saliency computation, where only the particular subset of the input image that is attended is consequently represented in higher visual systems [7]. The softmax operation can be construed as approximating this winner-take-all mechanism. The attention is consequently applied as element-wise scaling to F_{rep} to yield an attention modulated representation $F_{rep}^a = F_{rep} \odot A$.

Convolutional response model The convolutional response model maps the spatially pooled attention modulated features $\mathbf{f}_g = \sum_{i=1}^n F_{rep}^{(i)}$ to the neural representation space, reshapes them into coarse 3D feature maps and transforms them into an increasingly fine-grained volumetric neural activation pattern using trainable convolutions. This dramatically reduces the parameter count in comparison to linear response models with dense connections. Additionally, it captures spatial context and allows end-to-end optimization of the neural encoding model to predict high-resolution neural response, thereby alleviating the need for voxel sub-sampling or selection. The full sequence of feedforward computations in the convolutional response model are shown in the inset of Figure 1. The architecture of the convolutional response model is kept consistent across all CNN-based models to ensure a fair comparison.

2.1 Baselines and upper bounds

No attention We compared the performance of all attention-based models against a model with no attention modulation that spatially pools the feature representation as, $\mathbf{f}_g = \sum_{i=1}^n F_{rep}^{(i)}$ (denoted as ‘No attention’). We implemented another baseline that uses the full feature map directly (instead of spatial pooling) as a flattened input to the convolutional response model. Due to computational/memory

constraints, we had to reduce the dimensionality of the fully connected layer (to 256 units instead of 1024) in the convolutional response model for this encoding method. This model is henceforth denoted as ‘No pooling’.

Center-weighted attention To further assess the usefulness of a learned attention network, we derive a stimulus-independent attention map (A_C) based on averaging across all eye gaze data in the training set, using Gaussian kernel density estimation. This essentially amounts to center-weighted attention (see Supplementary) since fixation locations on average are biased towards the center of an image [16]. The standard deviation of the Gaussian kernel is chosen to maximize log-likelihood on the validation set and is consequently set to 20.

Gaze-weighted attention We derive attention maps for every input frame from the eye gaze coordinates observed for the respective frame across different subjects. The human fixation maps are converted into attention maps A_G by blurring with a Gaussian kernel of same standard deviation as the center-weighted attention model. The resulting attention maps in the original input image space are subsequently resized to the spatial dimensions of F_{rep} and renormalized. Since these stimulus-specific attention maps are derived from actual human gaze information, they likely represent an upper bound in neural encoding performance among all attention-based models.

Linear models To date, neural encoding models in all prior work employ a linear response model with appropriate regularization on the regression weights. To compare against this dominant approach, we extract global average pooled (no-attention) features as well as pooled attention modulated features for both non-trainable attention schemes (center-weighted and gaze-weighted attention) as described above, to present to the linear regressor. We apply l_2 regularization on the regression coefficients and adjust the optimal strength of this penalty λ through cross-validation using 10 log-spaced values in $\{1e-5, 1e5\}$. In later sections, we denote the performance of the above models as ‘No attention (linear)’, ‘Center-weighted attention (linear)’ and ‘Gaze-weighted attention (linear)’ respectively.

2.2 Training procedure

All parameters were optimized to minimize the *mean squared error* between the predicted and target fMRI response using Adam [17] for 25 epochs with a learning rate of 1e-4. Validation curves were monitored to ensure convergence and hyperparameters were optimized on the validation set.

2.3 Evaluation

Neural encoding We evaluated the performance of all encoding models on the test movie by computing the *Pearson’s correlation coefficient* (R) between the predicted and measured fMRI response at each voxel. Since we are only interested in the stimulus-driven response, we isolate voxels that exhibit high inter-group correlations over all training movies. Inter-group correlation (“synchrony”) values were computed by splitting the population into half and computing correlations between the mean response time-course of each group (comprising 79 subjects) at every voxel. We employed a liberal threshold of 0.15 for this correlation value to consider a voxel as “synchronous” [18]. Finally, to summarize the prediction accuracy across the stimulus-driven cortex, we compute the mean correlation coefficient across the synchronous cortex voxels by varying the “synchrony” thresholds. For region level analysis, ROIs were extracted using a population-wide multi-modal parcellation of the human cerebral cortex, namely the HCP MMP parcellation [19].

Saliency prediction Next, we wanted to assess if the learned attention model was indeed looking at meaningful locations in input images while predicting neural responses. To address this question and put the learned attention schemes in perspective, we assessed the agreement of predicted saliency maps with human fixation maps for every frame in the test movie. Besides a qualitative evaluation, we computed quantitative metrics for comparing the predicted saliency maps against popular fixation (or saliency) prediction approaches. These include: (i) Itti-Koch [20]: a biologically plausible model of saliency computation that assigns pixel-level conspicuity values based on multi-scale low-level feature maps (intensity, color, orientation) computed via center-surround like operations similar to visual receptive fields, (ii) Deepgaze-II model [21]: a deep neural network based approach that extracts high-level features from a pre-trained image recognition architecture (VGG19) as input to a readout network that is subsequently trained to predict fixations using supervision from gaze data,

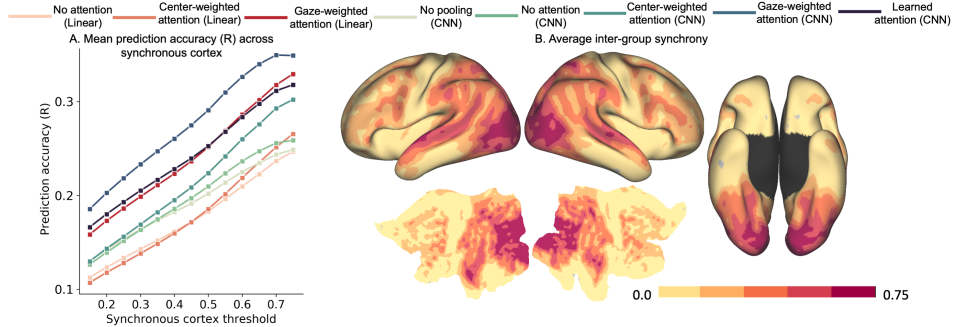


Figure 2: Quantitative evaluation of all models. (A) depicts mean correlation values across the synchronous, (i.e., stimulus-driven) cortex defined at a range of synchrony thresholds ([0.15,0.75]). Each point thus reflects the mean prediction accuracy for a model across all voxels within synchronous cortex defined by a threshold value (x-axis). (B) depicts the inter-group correlation (synchrony) values across the entire human cerebral cortex.

and (iii) Intensity contrast features (ICF) model [21]: a low-level saliency computation model that uses the same readout architecture as the Deepgaze-II model, but on low-level intensity and intensity contrast feature maps as opposed to high-level features. Additionally, we also report evaluation metrics for the center-weighted saliency map. We note that the Deepgaze-II and ICF models were trained with eye-tracking supervision on the MIT1003 saliency dataset [22].

Developing metrics for saliency evaluation is an active area of research and several different metrics have been proposed that often exhibit discrepant behavior [23]. We report the most commonly used metrics in saliency evaluation [23], including, (i) Similarity or histogram intersection (SIM), (ii) Pearson’s correlation coefficient (CC), (iii) Normalized scanpath saliency (NSS), (iv) Area under the ROC curve (AUC) and (v) Shuffled AUC (sAUC). Following [24], we used log-density predictions as saliency maps to compute all evaluation metrics.

2.4 Dataset

We study high-resolution 7T fMRI (TR = 1s, voxel size = 1.6 mm isotropic) recordings of 158 participants from the Human Connectome Project (HCP) movie-watching database while they viewed 4 audio-visual movies in separate runs [12, 25]. Each movie scan was about 15 minutes long, comprising multiple short clips from popular Hollywood movies and/or vimeo. Eye gaze locations of subjects were also recorded simultaneously at 1000Hz and resampled to 24Hz to match the video frame acquisition rate. A standard pipeline was used to preprocess all fMRI data, which includes motion and distortion correction, high-pass filtering, head motion effect regression using Friston 24-parameter model, automatic removal of artifactual timeseries identified with Independent Component Analysis (ICA) as well as nonlinear registration to the MNI template space [26, 25]. Since the present study focuses on the development of population-wide predictive models, we averaged the response for each frame across subjects to obtain a single fMRI volume that represents the population average brain activation in response to that frame. After discarding rest periods as well as the first 10 seconds of every movie segment, we used about 12 minutes of audio-visual stimulation data per movie paired with the corresponding fMRI response and fixation data for analysis. We extract the last frame of every second of the video as a $720 \times 1280 \times 3$ RGB input to present as stimulus to the neural encoding models. The output is the predicted response across the entire brain, represented as a volumetric image of dimensions $113 \times 136 \times 113$. We estimate a hemodynamic delay of 4 sec using regression based encoding models (see Supplementary), as the response latency that yields highest encoding performance. Thus, all proposed and baseline models are trained to use the above stimuli to predict the fMRI response 4 seconds *after* the corresponding stimulus presentation. We train and validate our models on three movies using a 9:1 train-val split and leave the fourth movie for independent testing. This yields 2000 training, 265 validation and 699 test stimulus-response pairs.

3 Results

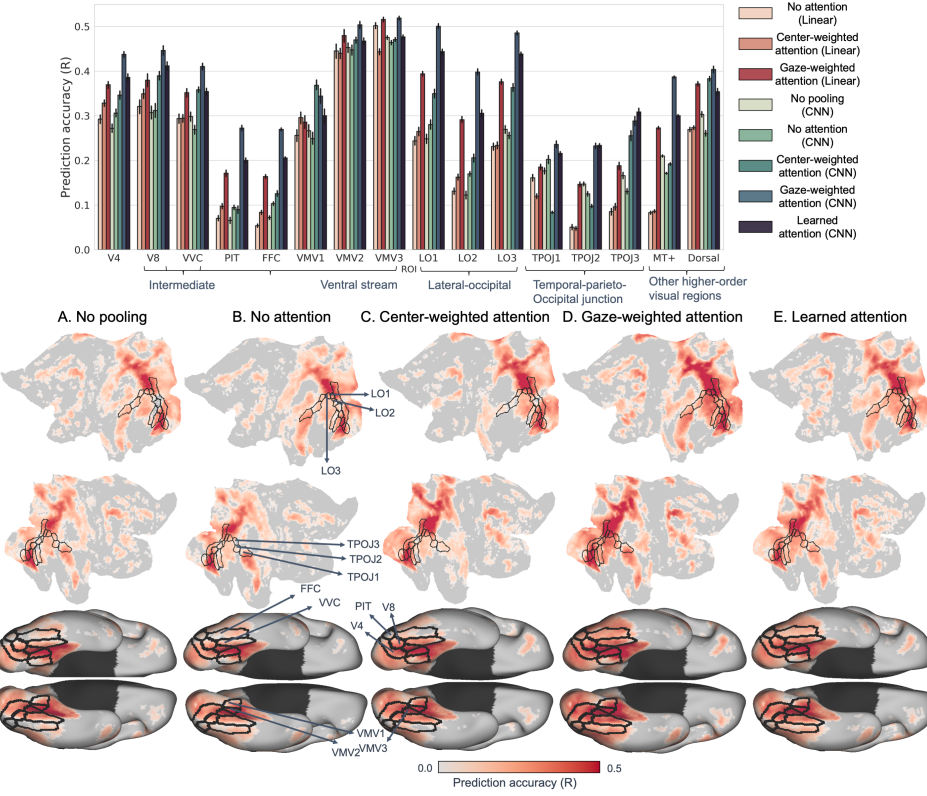


Figure 3: Top: ROI-level analysis Mean correlation values across intermediate (V4), higher visual areas in the inferotemporal cortex and its neighborhood and other higher-level visual regions (Dorsal, MT+) as described in the HCP MMP parcellation [19]. Error bars represent 95% confidence intervals around mean estimates computed using bootstrap sampling. **(A)-(E) Prediction accuracy across the cortical surface for all deep CNN-based models.** Statistical significance of individual voxel predictions is computed as the p-value of the obtained sample correlation coefficient for the null hypothesis of uncorrelatedness (i.e., true correlation coefficient is zero) under the assumptions of a bivariate normal distribution. Only significantly predicted voxels ($p < 0.05$, FDR corrected) for each method are colored on the surface. Prediction accuracy maps for encoding methods with linear response models are provided in the Supplementary.

Incorporating gaze-weighted attention significantly improves neural response prediction. We first examined whether attention weighted pooling helps to improve response predictions. Figure 2 shows the mean prediction accuracy across the entire synchronous cortex for all models considered in this study. We find that the ‘gaze-weighted attention’ model significantly outperforms the ‘no attention’ model for both linear ($\sim 40\%$ improvement among all voxels with synchrony > 0.15), as well as convolutional response model ($\sim 47\%$ improvement among all voxels with synchrony > 0.15). The attention maps result in amplification of features of attended locations along with suppression of other irrelevant information. This re-scaling of features before pooling using fixation patterns obtained from eye-tracking data remarkably improves neural encoding performance across large areas of the cortex, suggesting that neural responses are indeed dominated by sensory signals at attended locations. Although we employed a convolutional response model primarily for computational efficiency in predicting a high-resolution (113x136x113) whole-brain neural response, we also observed a small improvement in neural encoding with this response model in comparison to a linear response model.

Trainable attention model outperforms models with no attention or center-weighted attention In addition to improving neural response prediction, the convolutional response model renders end-to-end training of encoding models on whole-brain neural data feasible by dramatically reducing the number of free parameters in comparison to linear response models. In this study, we exploited this increased parameter efficiency to co-train an attention network on top of a pre-trained representation

Table 1: Evaluation against saliency prediction models. Mean and standard errors for each metric are reported. Best results are bolded.

Model	SIM \uparrow	CC \uparrow	NSS \uparrow	AUC \uparrow	sAUC \uparrow
Itti-Koch	0.318 ± 0.002	0.325 ± 0.004	1.010 ± 0.014	0.795 ± 0.004	0.537 ± 0.006
ICF	0.291 ± 0.002	0.190 ± 0.007	0.646 ± 0.023	0.665 ± 0.006	0.647 ± 0.005
Center-weighted	0.327 ± 0.002	0.350 ± 0.004	1.074 ± 0.013	0.803 ± 0.003	0.496 ± 0.006
Deepgaze-II	0.359 ± 0.003	0.420 ± 0.005	1.425 ± 0.025	0.808 ± 0.004	0.713 ± 0.004
Ours	0.392 ± 0.004	0.403 ± 0.010	1.375 ± 0.041	0.754 ± 0.006	0.645 ± 0.006

network (while freezing the representation network) for the goal of neural response prediction. As shown in Figure 2, the encoding model with learned attention surpasses models with no pooling, no attention or center-weighted attention in mean prediction accuracy across the synchronous cortex as well across most ROIs involved in object processing. This suggests that even with no eye-tracking data, as is the case with majority movie-watching fMRI datasets, modelling visual attention can still be beneficial in response prediction. The improvements are most apparent in ventral stream regions such as the Fusiform Face Complex (FFC) and PIT Complex, as well as objective-selective parts of the lateral occipital complex (LO1, LO2, LO3) (Figure 2). Studies in visual perception have shown that these lateral occipital areas respond more strongly to intact objects than scrambled objects or textures, providing strong evidence for their role in object recognition as well as object shape perception [27, 28, 29]. Accuracy in another group of areas within the temporo-parieto-occipital junction, which is known to be involved in visual object recognition as well as representation of facial attributes such as the intensity of facial expressions [30], is similarly improved with the trained attention network. In addition to these areas, we also observe some improvement in neural encoding performance in other higher order processing regions across the dorsal visual stream, motion-sensitive visual regions (MT+ complex) and their neighboring visual areas (Figure 3). We also trained the proposed and baseline models on representations of other randomly selected deep layers within the ResNet-50 architecture and observed a similar benefit of attention modulation across different layers (see Supplementary). Further, a representational similarity analysis comparing non-modulated and attention modulated representations of different layers across popular architectures showed that models that explain stimulus-dependent human fixation patterns are able to better account for the representational geometry of neural responses across intermediate and higher visual object processing areas (see Supplementary). Taken together, these findings provide further support for the utility of attention modelling in neural encoding approaches. In addition to improving accuracy, the attention model further affords interpretability by highlighting salient locations within the input image that are being employed to make response predictions.

Learned attention policies correspond remarkably well with human fixation maps. Figure 4 depicts saliency maps predicted by the trained attention network on sampled frames from the test movie. This qualitative assessment indicates that the proposed neural encoding model learns attention policies that are consistent with human fixation maps. Since attention is learned on top of high-level features, the model learns to focus on high-level stimuli features such as the presence of faces, hands and more conspicuous objects likely to direct attention in natural scenes. A closer look at incongruent cases indicates that images where the model fails to track human fixations are often highly complex scenes, where fixations may be driven by contextual knowledge of previous movie frames (Figure 4, top-right) or auditory signals, e.g., who the speaker is, etc. (Figure 4, bottom-right).

Table 1 shows quantitative metrics that compare the quality of saliency maps computed by benchmark models trained to predict gaze on our data. We also listed the performance of the attention network that was merely trained on fMRI data, and not eye gaze data. We note that our attention network performs on par with popular fixation prediction models that are trained directly on the task of saliency prediction in a supervised manner (ICF and Deepgaze-II). This trend holds for almost all saliency evaluation metrics, as shown in Table 1. This observation is particularly interesting given that the attention network is trained using supervision from neural response prediction only, without any information about gaze coordinates.

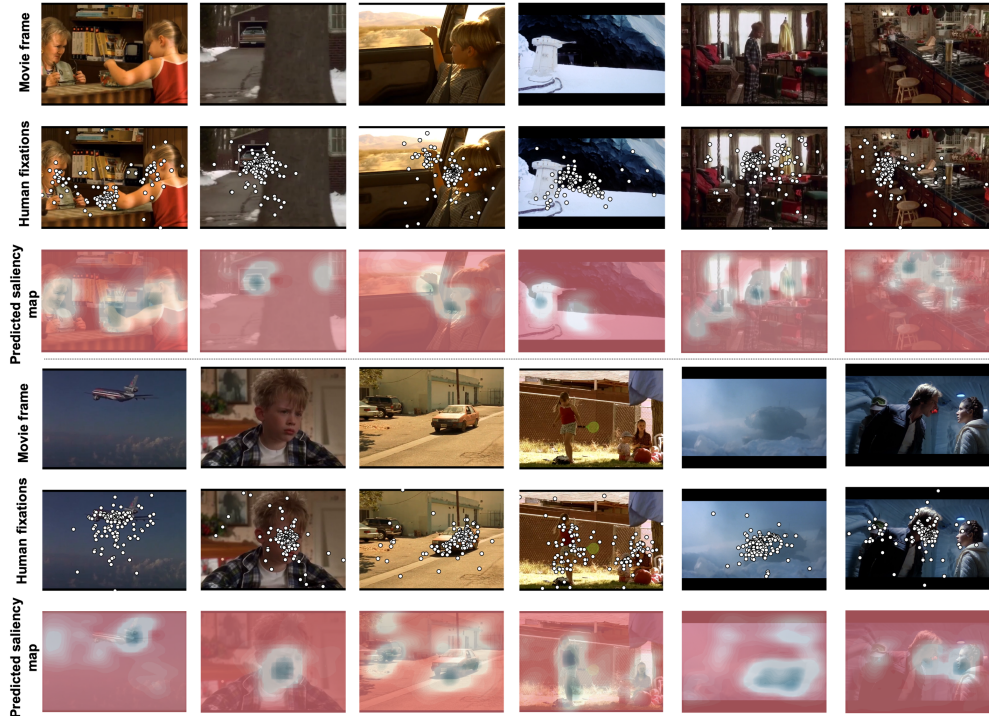


Figure 4: **Qualitative assessment of saliency (log-density) maps.** Top row shows sampled frames from the test movie, middle row shows human fixation maps overlaid on the corresponding frame, bottom row shows saliency maps predicted by the attention network of the proposed neural encoding model.

4 Discussion and Conclusion

In the present study, we demonstrate that encoding models with visual attention, whether explicitly estimated from human fixation maps or modelled using a trainable soft-attention scheme, yield significant improvements in neural response prediction accuracy over non-attention based counterparts. We observe consistent improvements across most high-level visual processing regions, suggesting that unattended portions of an input image may likely have little effect on neural representations in these regions. Loosely, this aligns well with Treisman’s feature integration theory [31], which proposes that integrated object representations are only formed for attended locations. In addition to improving response prediction accuracy, inclusion of visual attention within neural encoding models promises a better understanding of spatial selection and its influence on neural representations and perceptual processing.

The saliency of a stimulus often depends on the context within which it is presented and attentional selection strategies can be modulated by task demands [8]. Thus, in movie watching, future neural encoding models should also capture the sequence of frames, rather than isolated frames, and the audio track in modeling attention.

Beyond advancing our understanding of sensory perception, neural encoding models have potential for real-world applications, most obviously for brain-machine interface. Additionally, an improved understanding of the link between sensory stimuli and evoked neural activation patterns can provide opportunities for neural population control, for e.g., by synthetically designing stimuli to elicit a specific neural activation pattern [32].

Our study provides a first attempt in capturing visual attention within neural encoding models. We see several opportunities for extending this work. In the present framework, we employed attention as a masking strategy to filter out clutter and retain information from only the most relevant (i.e. attended) parts of an image. It would be interesting to study how and where the features of ignored stimuli (i.e. the stimuli that doesn’t get past the attentional bottleneck) are encoded. Further, here, we

modeled attention on top of high-level semantic features. In principle, the attention network can be implemented on top of any level within the representation network hierarchy, including lower stages and understanding where attention computations leads to best neural prediction accuracy and/or agreement with human fixation maps could be a worthwhile exploration. In the future, we aim to further explore novel ways of incorporating attention within neural encoding models.

Broader Impact

Understanding the link between sensory stimulation and evoked neural activity in humans as revealed with encoding models, can provide foundations for developing novel therapies. Viewed in this regard, an improved understanding of information processing in the brain has tremendous potential. However, encoding models can be very sensitive to biases in the training set. Our models were trained using data from the Human Connectome Project database. While this large-scale project has made a lot of valuable data publicly available to the scientific community for studying brain structure and function, it is important to consider the representational bias in the dataset. For instance, the data we analyzed is exclusively limited to a young adult population. Such biases can possibly lead to poorer generalization of models trained with these large-scale datasets on other population groups that are inadequately represented. Once these encoding models are ripe for therapeutic applications, this dataset bias could prevent under-represented groups from deriving the benefits of a useful technology, resulting in uneven access across populations. Given these considerations, it is important to address potential representation biases in fMRI datasets and develop solutions for improving diversity and inclusion. More generally, fMRI studies involving human subjects can raise a wide range of other ethical issues as well, including data privacy issues and informed consent.

Further, one should be cautious about the deployment of attention or gaze prediction models in applications such as advertising. Given the value of eye tracking based attention in marketing spaces, public policy notices or political campaigns, it is important to be wary of a malicious use of these attention prediction methods for profit-seeking or by ill-intentioned parties seeking to further their own agendas. These applications regard attention as a commodity to be captured and the adopted technologies can be used to manipulate users in subtle ways. An improved understanding about the link between stimuli and perceptual processing in the brain, as provided with encoding models, can also be exploited to further design or identify stimuli likely to elicit a specific emotional or cognitive response. The fact that these technologies can be deployed without the targeted individual's knowledge or consent indicates it is important to protect users from the vulnerabilities exploited by these agents.

Acknowledgements

This work was supported by NIH grants R01LM012719 (MS), R01AG053949 (MS), R21NS10463401 (AK), R01NS10264601A1 (AK), the NSF NeuroNex grant 1707312 (MS), the NSF CAREER 1748377 grant (MS) and Anna-Maria and Stephen Kellen Foundation Junior Faculty Fellowship (AK).

References

- [1] S. Sonkusare, M. Breakspear, and C. Guo. Naturalistic Stimuli in Neuroscience: Critically Acclaimed. *Trends Cogn. Sci. (Regul. Ed.)*, 23(8):699–714, Aug 2019.
- [2] D. L. Yamins, H. Hong, C. F. Cadieu, E. A. Solomon, D. Seibert, and J. J. DiCarlo. Performance-optimized hierarchical models predict neural responses in higher visual cortex. *Proc. Natl. Acad. Sci. U.S.A.*, 111(23):8619–8624, Jun 2014.
- [3] U. Guclu and M. A. van Gerven. Deep Neural Networks Reveal a Gradient in the Complexity of Neural Representations across the Ventral Stream. *J. Neurosci.*, 35(27):10005–10014, Jul 2015.
- [4] Alexander J.E. Kell, Daniel L.K. Yamins, Erica N. Shook, Sam V. Norman-Haignere, and Josh H. McDermott. A Task-Optimized Neural Network Replicates Human Auditory Behavior, Predicts Brain Responses, and Reveals a Cortical Processing Hierarchy. *Neuron*, 98(3):630–644.e16, may 2018.
- [5] John T. Serences and Steven Yantis. Selective visual attention and perceptual coherence. *Trends in Cognitive Sciences*, 10:38–45, 2006.
- [6] Sabine Kastner and Leslie G. Ungerleider. Mechanisms of visual attention in the human cortex. *Annual review of neuroscience*, 23:315–41, 2000.
- [7] Jochen Braun, Christof Koch, and Joel L. Davis. Visual attention and cortical circuits. In *Visual attention and cortical circuits*, 2001.
- [8] Laurent Itti and Christof Koch. Computational modelling of visual attention. *Nature Reviews Neuroscience*, 2:194–203, 2001.
- [9] Tomaso Poggio and Fabio Anselmi. Visual cortex and deep networks: Learning invariant representations. In *Visual Cortex and Deep Networks: Learning Invariant Representations*, 2016.
- [10] James E. Hoffman and Baskaran Subramaniam. The role of visual attention in saccadic eye movements. *Perception & Psychophysics*, 57:787–795, 1995.
- [11] Thomas P O’Connell and Marvin M. Chun. Predicting eye movement patterns from fmri responses to natural scenes. *Nature Communications*, 9, 2018.
- [12] M. F. Glasser, S. N. Sotiroopoulos, J. A. Wilson, T. S. Coalson, B. Fischl, J. L. Andersson, J. Xu, S. Jbabdi, M. Webster, J. R. Polimeni, D. C. Van Essen, and M. Jenkinson. The minimal preprocessing pipelines for the Human Connectome Project. *Neuroimage*, 80:105–124, Oct 2013.
- [13] Kaiming He, Xiangyu Zhang, Shaoqing Ren, and Jian Sun. Deep residual learning for image recognition. *2016 IEEE Conference on Computer Vision and Pattern Recognition (CVPR)*, pages 770–778, 2015.
- [14] Jia Deng, Wei Dong, Richard Socher, Li-Jia Li, Kai Li, and Fei-Fei Li. Imagenet: A large-scale hierarchical image database. *2009 IEEE Conference on Computer Vision and Pattern Recognition*, pages 248–255, 2009.
- [15] Haiguang Wen, Junxing Shi, Yizhen Zhang, Kun Han Lu, Jiayue Cao, and Zhongming Liu. Neural encoding and decoding with deep learning for dynamic natural vision. *Cerebral Cortex*, 28(12):4136–4160, dec 2018.
- [16] Po-He Tseng, Ran Carmi, Ian G. M. Cameron, Douglas P. Munoz, and Laurent Itti. Quantifying center bias of observers in free viewing of dynamic natural scenes. *Journal of vision*, 9 7:4, 2009.
- [17] Diederik P. Kingma and Jimmy Ba. Adam: A method for stochastic optimization. *CoRR*, abs/1412.6980, 2014.
- [18] U. Hasson, Y. Nir, I. Levy, G. Fuhrmann, and R. Malach. Intersubject synchronization of cortical activity during natural vision. *Science*, 303(5664):1634–1640, Mar 2004.
- [19] M. F. Glasser, T. S. Coalson, E. C. Robinson, C. D. Hacker, J. Harwell, E. Yacoub, K. Ugurbil, J. Andersson, C. F. Beckmann, M. Jenkinson, S. M. Smith, and D. C. Van Essen. A multi-modal parcellation of human cerebral cortex. *Nature*, 536(7615):171–178, 08 2016.
- [20] Laurent Itti, Christof Koch, and Ernst Niebur. A model of saliency-based visual attention for rapid scene analysis. *IEEE Trans. Pattern Anal. Mach. Intell.*, 20:1254–1259, 2009.

- [21] Matthias Kümmerer, Thomas S. A. Wallis, Leon A. Gatys, and Matthias Bethge. Understanding low- and high-level contributions to fixation prediction. *2017 IEEE International Conference on Computer Vision (ICCV)*, pages 4799–4808, 2017.
- [22] Zoya Bylinskii, Tilke Judd, Ali Borji, Laurent Itti, Frédo Durand, Aude Oliva, and Antonio Torralba. Mit saliency benchmark. <http://saliency.mit.edu/>.
- [23] Zoya Bylinskii, Tilke Judd, Aude Oliva, Antonio Torralba, and Frédo Durand. What do different evaluation metrics tell us about saliency models? *IEEE Transactions on Pattern Analysis and Machine Intelligence*, 41:740–757, 2016.
- [24] Matthias Kümmerer, Thomas S. A. Wallis, and Matthias Bethge. Information-theoretic model comparison unifies saliency metrics. *Proceedings of the National Academy of Sciences of the United States of America*, 112(52):16054–9, 2015.
- [25] D. C. Van Essen, K. Ugurbil, E. Auerbach, D. Barch, T. E. Behrens, R. Bucholz, A. Chang, L. Chen, M. Corbetta, S. W. Curtiss, S. Della Penna, D. Feinberg, M. F. Glasser, N. Harel, A. C. Heath, L. Larson-Prior, D. Marcus, G. Michalareas, S. Moeller, R. Oostenveld, S. E. Petersen, F. Prior, B. L. Schlaggar, S. M. Smith, A. Z. Snyder, J. Xu, and E. Yacoub. The Human Connectome Project: a data acquisition perspective. *Neuroimage*, 62(4):2222–2231, Oct 2012.
- [26] A. T Vu, K. Jamison, M. F. Glasser, S. M. Smith, T. Coalson, S. Moeller, E. J. Auerbach, K. Ugurbil, and E. Yacoub. Tradeoffs in pushing the spatial resolution of fMRI for the 7T Human Connectome Project. *Neuroimage*, 154:23–32, 07 2017.
- [27] K. Grill-Spector, Z. Kourtzi, and N. Kanwisher. The lateral occipital complex and its role in object recognition. *Vision Res.*, 41(10-11):1409–1422, 2001.
- [28] Zoe Kourtzi and Nancy Kanwisher. Cortical regions involved in perceiving object shape. *The Journal of neuroscience : the official journal of the Society for Neuroscience*, 20(9):3310–8, 2000.
- [29] Jonas Larsson and David J. Heeger. Two retinotopic visual areas in human lateral occipital cortex. *The Journal of neuroscience : the official journal of the Society for Neuroscience*, 26(51):13128–42, 2006.
- [30] Alessandro De Benedictis, Hugues Duffau, Beatrice Paradiso, Enrico Grandi, Sergio Balbi, Enrico Granieri, Enzo Colarutto, Franco Chioffi, Carlo Efisio Marras, and Silvio Sarubbo. Anatomo-functional study of the temporo-parieto-occipital region: dissection, tractographic and brain mapping evidence from a neurosurgical perspective. *Journal of anatomy*, 225(2):132–51, 2014.
- [31] Anne Treisman and G. A. Gelade. A feature-integration theory of attention. *Cognitive Psychology*, 12:97–136, 1980.
- [32] Pouya Bashivan, Kohitij Kar, and James J. DiCarlo. Neural population control via deep image synthesis. *bioRxiv*, 2018.
- [33] Nikolaus Kriegeskorte, Marieke Mur, and Peter A. Bandettini. Representational similarity analysis – connecting the branches of systems neuroscience. *Frontiers in Systems Neuroscience*, 2, 2008.
- [34] Seyed-Mahdi Khaligh-Razavi and Nikolaus Kriegeskorte. Deep supervised, but not unsupervised, models may explain cortical representation. *PLoS Computational Biology*, 10, 2014.

Supplementary Information

Model comparison across randomly selected layers

Here, we wanted to examine if the learned attention model would lead to performance improvements in neural response prediction across other deep layers as well. We trained all 8 models using stimuli representations F_{rep} from 2 randomly selected layers in the res5 block of the pre-trained ResNet-50 architecture, namely ‘add_14’ and ‘res5c_branch2b’², henceforth denoted as ‘Random ResNet-50 layer 1’ and ‘Random ResNet-50 layer 2’ respectively. Figure S1 shows the prediction accuracy across the synchronous cortex on the held-out movie for all models. We again observe that the learned attention model performs favorably against models with no attention, no pooling or center-weighted attention. Further, the gaze-weighted attention method outperforms all other methods employing the same response model (linear or convolutional), consistent with our previous findings.

Representational similarity analysis

Representational similarity analysis (RSA) is a popular framework to compare representations of a computational model against cortical representations [33, 34]. It can be used to directly measure a computational model’s ability to explain the representational geometry in neuronal responses. Here, we wanted to assess the impact of attention modulation on a computational model’s alignment to brain responses for a wider range of model layers and architectures. Given stimuli from the held-out movie (699 frames) and the corresponding response (after hemodynamic lag), we implemented the following procedure for time-continuous RSA: (i) We computed Pearson’s correlation distance ($1-R$) between the response vectors for every pair of test frames to obtain the representational dissimilarity matrix (RDM) of neural responses. The dissimilarity matrices are averaged across subjects to yield a population-averaged ‘neural’ RDM. The region of interest (ROI) mask for extracting response vectors to estimate neural RDMs was derived from all voxels in intermediate (V4), ventral visual stream and lateral occipital ROIs. Responses of all voxels were normalized using z-scores before computing the dissimilarity matrix. (ii) We extracted model representations from intermediate layers of 3 pre-trained (ImageNet) architectures, namely ResNet-50 (res2, res3, res4, res5), VGG-16 (maxpool1, maxpool2, maxpool3, maxpool4, maxpool5) and AlexNet (conv1, conv2, conv3, conv4, conv5). For each of these representations, we further computed attention modulated representations using attention maps computed with each saliency prediction method as described above. For the Itti-Koch model, we used normalized saliency as the attention map. For all remaining saliency models, we used probabilistic density predictions as attention maps. All attention maps were resized to the spatial dimensions of the respective layer for this computation. Representational vectors were compared pair-wise in terms of their Pearson correlation distance ($1-R$) to obtain the ‘model’ RDM. (iii) Finally, we compared the compatibility of the neural and model RDMs by using a rank correlation measure (Kendall’s τ_A).

As shown in Figure S2, prioritized selection of stimulus features based on saliency significantly improves the correlation of model RDMs with neural RDMs. This trend holds for most models and layers, suggesting that the benefits of attentional masking are not restricted to forward encoding models alone, but may be more universal. Further, we find that models that better explain stimulus-dependent human fixation patterns (such as Deepgaze-II or the learned attention model) are able to better account for the representational geometry of neural responses across higher visual object processing areas.

Regions of interest (ROI)

We employed the HCP MMP parcellation for all ROI-level analysis. Dorsal and ventral visual stream ROIs as well as MT+ ROIs in Figure 3 (main text) were derived from the explicit stream segregation and categorization described in the HCP MMP parcellation [19] and are defined here in Table S1 for quick reference.

Center-weighted attention

Figure S3 depicts the center-weighted saliency map used in all center-weighted attention models. We also report per-movie eye tracking statistics therein from all frames used for training or testing

²Notation from pre-trained ResNet-50 model: <https://keras.io/api/applications/resnet/>

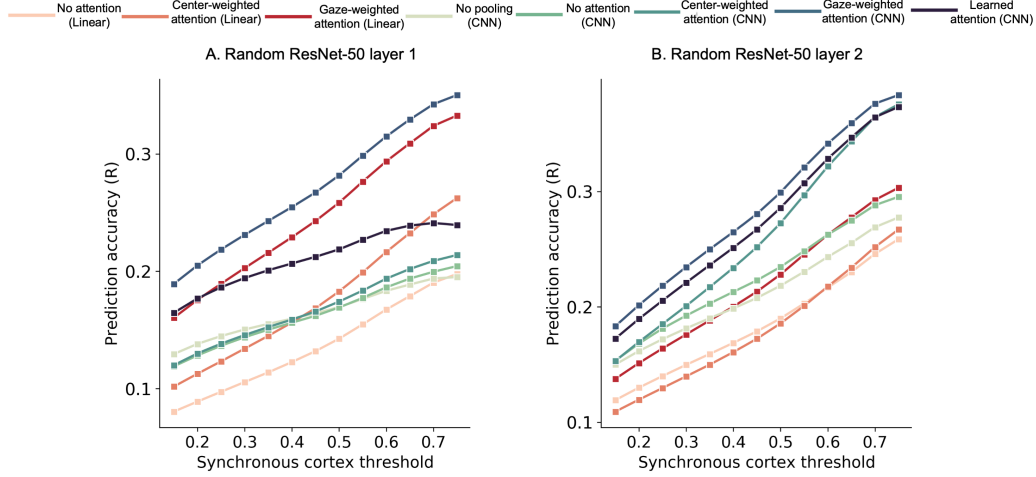


Figure S1: **Quantitative evaluation.** Mean correlation values across the synchronous, (i.e., stimulus-driven) cortex defined at a range of synchrony thresholds ([0.15,0.75]). Each point thus reflects the mean prediction accuracy for a model across all voxels within synchronous cortex defined by a threshold value (x-axis).

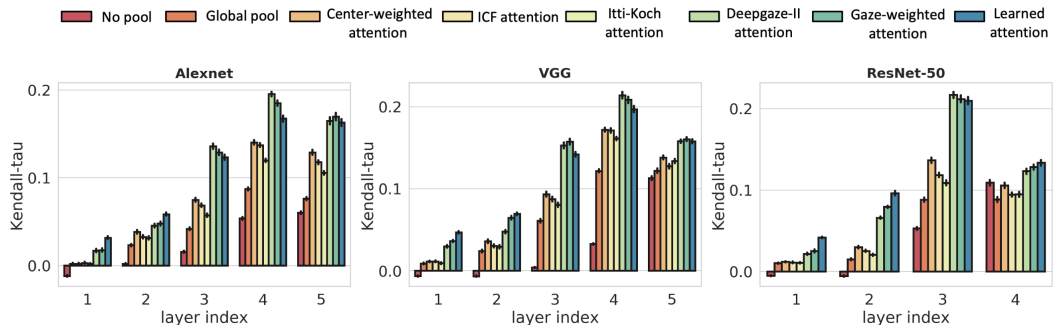


Figure S2: **Representational similarity analysis(RSA).** y-axis measures the agreement between ‘model’ RDMs and ‘neural’ RDMs based on their rank correlation measure. x-axis is use to index the layer (index 1 refers to the earliest layer of the architecture) and the saliency method used for attention masking of the features before pooling.

Table S1: ROI categorization

Group	ROIs
Dorsal	V3A, V3B, V6, V6A, V7, IPS1
Ventral	V8, VVC, PIT, FFC, VMV1-3
MT+	MT, MST, V4t, FST
Lateral occipital	LO1, LO2, LO3

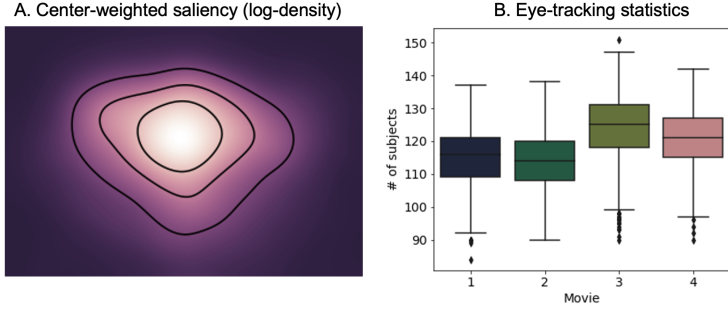


Figure S3: **A. Center-weighted saliency map and B. Eye tracking statistics**

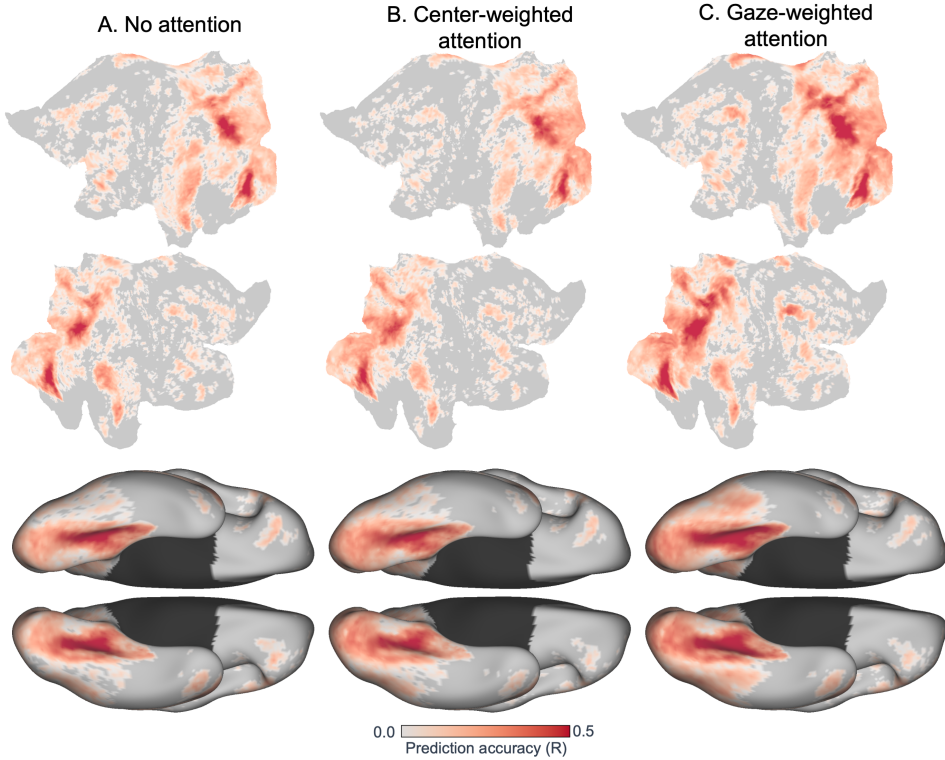


Figure S4: **Prediction accuracy across the cortical surface for all methods using linear response models.** Statistical significance of individual voxel predictions is computed as the p-value of the obtained sample correlation coefficient for the null hypothesis of uncorrelatedness (i.e., true correlation coefficient is zero) under the assumptions of a bivariate normal distribution. Only significantly predicted voxels ($p < 0.05$, FDR corrected) for each method are colored on the surface.

the models. We note that not all subjects had eye tracking measurements for every frame in the movies. Figure S3B shows the number of subjects for which eyetracking data was available per movie (distribution across frames). This suggests that despite the missing data, most frames among all training and testing movies (MOVIE 4) had recorded gaze coordinate measurements from $\sim 110\text{-}130$ subjects.

Voxel-wise prediction accuracy (R) of linear models

Figure S4 depicts the prediction accuracy across the cortical surface for all methods employing linear response models that were considered in this study. As can be seen clearly, just as in methods with

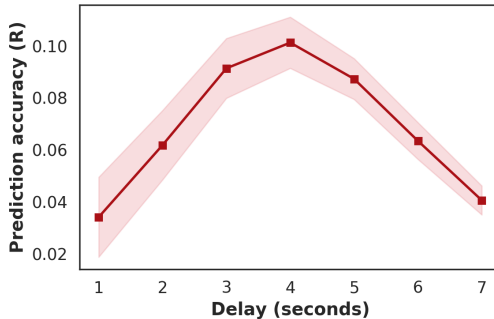


Figure S5: Hemodynamic response delay. 5-fold cross-validated prediction accuracy (R) of the simple ('No attention') model on the training dataset. Error margins are computed from the standard deviation of prediction accuracy across the 5 folds.

CNN response models, gaze-weighted attention significantly improves prediction accuracy across most higher order visual areas over models with no attention or center-weighted attention.

Estimating hemodynamic (BOLD) response delay

fMRI BOLD response delay was estimated using the baseline 'No attention (Linear)' encoding model due to its computational efficiency in comparison to encoding models employing convolutional response models. The input to these models was the 2048 dimensional (average pooled) representation of the stimuli, and the output was the evoked fMRI response across the synchronous cortex (i.e., voxels with synchrony >0.15) at different lags (1-7 seconds) from the stimulus. Thus, the output is a 160900-D vector corresponding to the fMRI response. All models were trained with 5-fold cross-validation using the stimulus-response pairs from the *training* dataset only.

Based on Figure S5, we estimated a response delay of 4 seconds, as this lag consistently yielded the maximum prediction accuracy across 5-fold cross validation. Thus, all encoding models described in the main text were trained to predict fMRI response *after* 4 seconds of stimulus presentation.

Predicted saliency maps for the entire held-out movie

The following figures show the fixation maps and corresponding saliency maps predicted by the attention network of the proposed neural encoding model for frames sampled every 4 seconds from the held-out movie.

